



ChemComm

**Tuning water adsorption, stability, and phase in Fe-MIL-101
and Fe-MIL-88 analogs with amide functionalization**

Journal:	<i>ChemComm</i>
Manuscript ID	CC-COM-04-2021-002104.R1
Article Type:	Communication

SCHOLARONE™
Manuscripts

COMMUNICATION

Tuning water adsorption, stability, and phase in Fe-MIL-101 and Fe-MIL-88 analogs with amide functionalization

Received 00th January 20xx,
Accepted 00th January 20xx

Andrew Kuznicki,^a Gregory R. Lorzina^a and Eric D. Bloch^{*a}

DOI: 10.1039/x0xx00000x

Metal-organic frameworks (MOFs) of the MIL series of materials have been widely studied as a result of their high tunability and the diversity of structure types that exist for these typically M³⁺ containing frameworks. We explored the use of amide-functionalized ligands in the synthesis of Fe-MIL-101 as a means to tune the water stability and water vapor adsorption in this important class of frameworks. We further show that slow leaching of Fe from NdFeB magnets can afford MIL-101 or MIL-88 under various conditions where the phase of the framework is controlled by length of the carbon chains on amide substituents. NdFeB can also be used to prepare these materials at room temperature in the absence of additional metal salts.

Metal-organic frameworks (MOFs) have garnered a great deal of attention over the last few decades due to their high surface areas,¹ wide range of topologies,² and ease of modification.³ By utilizing judicious design principles, MOFs can be tuned for specific applications.^{4,5,6} Their ease of rational design is a result of their modular construction⁷ where ligand functionalization, which can take place before or after framework assembly,^{8,9} can be tuned to generate specific desired properties.¹⁰

One of the major drawbacks that has plagued many MOFs, particularly those based on carboxylic acid, is their relative lack of water stability due to protonation of weaker metal-carboxylate bonds.¹¹ Some carboxylate-based materials, however, including those featuring metal cations in higher oxidation states such as Zr⁴⁺ or M³⁺ (M = Al, Cr, Fe) have displayed excellent thermal, chemical, and hydrolytic stability. The chromium(III) variants of the well-known MIL (Materials Institute Lavoisier)¹² series of frameworks display excellent stability.¹³ Although this makes them attractive candidates for a broad range of applications, the chromium-oxygen bonds that endow the framework with high stability¹⁴ increases harshness of the synthetic conditions required to assemble the materials, often requiring high temperature and/or corrosive additives, such as HF, for synthesis.¹⁵ The nature of the synthetic conditions required to assemble these structures

may limit the number of functionalized analogs that can be easily isolated, however, they are highly stable toward post-synthetic modification strategies.¹⁶ While the chromium-based materials are highly promising, chromium is a well-known environmental hazard and regulatory restrictions may become an obstacle for its use in many future applications.¹⁷ Fortunately, the MIL-101 structure type is compatible with alternative metals, such as aluminum,¹⁸ vanadium,¹⁹ or iron.²⁰ Although MIL-101(Fe) is relatively stable, it is prone to hydrolysis,²¹ resulting in the breakdown of the framework under aqueous conditions. However, incorporation of functional groups into the structure can lead to increased chemical stability while simultaneously tuning the adsorptive properties to fit a particular application. In a straightforward manner, incorporation of amide functional groups onto the terephthalic acid backbone of aluminum-based MIL-series MOFs²² and UIO-66 via post-synthetic modification (PSM) can tune stability and adsorption properties. However, when relying on PSM to alter framework pore surface chemistry, complete conversion to the amide ligand can be difficult to achieve.²³

The work reported here focuses on constructing a variety of Fe-MIL-101-amide frameworks by modifying 2-aminoterephthalic acid before synthesizing the MOF in order to obtain a fully functionalized material. Multiple amide functional groups were used in order to probe the effects that these modifications have on water stability, as well as pore sizes and gas adsorption properties. Along with a liquid and vapor water stability study, the functionalized MOF were exposed to a range of acidic/basic conditions to better understand the effects pH has on the overall stability.

Numerous procedures have been reported for the synthesis of both Fe-MIL-101 and Cr-MIL-101 (see ESI for full synthetic procedures).²⁴ Although they are relatively straightforward, care must be taken to avoid competing phases for these frameworks, which include MIL-53 and MIL-88 (Figure 1). For the materials isolated here, the reaction of iron(III) chloride with terephthalic acid in DMF at 110 °C for 12 hours affords Fe-MIL-101 in high yield. Rather than hot ethanol washes, we employed DMF washes, as terephthalic acid is highly soluble in this solvent. We also utilized thorough dichloromethane washes after amide washing to facilitate

^a Department of Chemistry and Biochemistry, University of Delaware, Newark, Delaware 19716, United States. E-mail: edb@udel.edu

[†] Electronic Supplementary Information (ESI) available: detailed experimental procedures, adsorption isotherms, powder X-ray diffraction data. See DOI: 10.1039/x0xx00000x

activation of samples for water testing or gas adsorption analysis. Heating Cr-MIL-101 to 150 °C and Fe-MIL-101 to 120 °C afforded samples with BET (Langmuir) surface areas of 2603 (3940) and 2680 (3501) m²/g, respectively. These surface areas are in line with previously reported BET values which typically average 2276 m²/g for Cr-MIL-101 and 2686 for Fe-MIL-101.²⁵

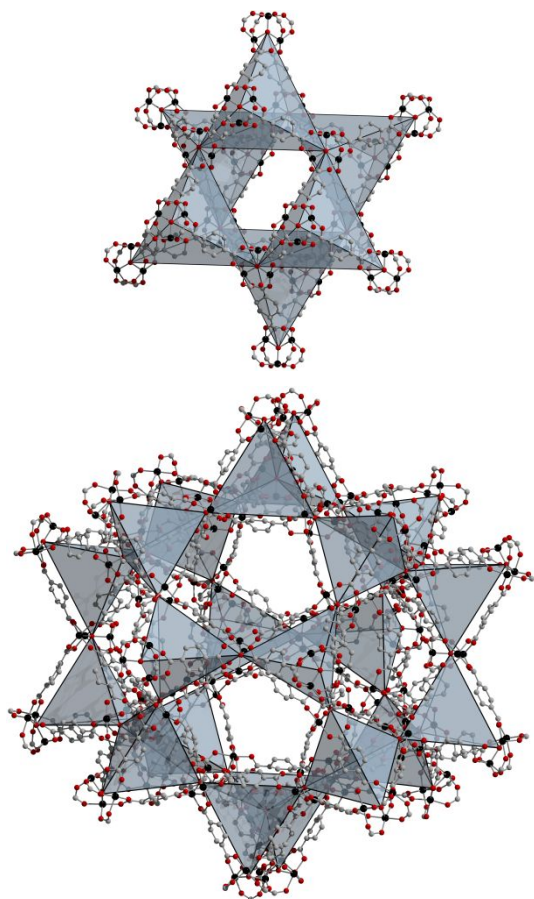


Fig. 1 A portion of the structures of Fe-MIL-88 (top) and Fe-MIL-101 (bottom) where black, red, and gray spheres represent iron, oxygen, and carbon atoms, respectively. The large pentagonal and hexagonal windows in the later are compatible with the installation of relatively bulky functional groups.

The high water stability of Cr-MIL-101 is well known. Indeed, the material prepared here shows no decrease in crystallinity after water exposure of at least two weeks at pH 5, 8, or 11 (Figure S14). In contrast, Fe-MIL-101 is nearly completely amorphous under the same conditions and displays significant structural degradation, as judged by PXRD, after less than two days of water exposure (Figure S14). Water vapor similarly has a tremendously negative effect on material properties as Fe-MIL-101 becomes nonporous after recording a vapor adsorption isotherm and attempting to reactivate the material (Figure S34). As the utility of amide-functionalization as a means to tune the stability, solubility, phase, or adsorption properties of metal-organic frameworks is well-documented, we targeted the installation of these groups on the interior surface of Fe-MIL-101 to determine the optimal trade-off between surface area and stability that invariably comes with the incorporation of functional groups inside the

pores of a MOF.

Although amide groups have been installed post-synthetically, we investigated the incorporation of these groups prior to material formation as a means to guarantee the level of functionalization as post-synthetic functionalization strategies can lead to incomplete reactions. Amide functionalized ligands are readily obtained via the straightforward reaction of butyryl chloride, 3,5-trimethylhexanoyl chloride, lauroyl chloride, or phenylacetyl chloride with 2-aminoterephthalic acid (H₂bdc-NH₂) cleanly affording the ligands shown in Figure 2 in high yield. The synthetic route to Fe-MIL-101 is broadly applicable to yield functionalized frameworks via reaction with functionalized ligands as framework syntheses proceed regardless of the nature of functional group incorporation. Powder X-ray diffraction confirms the successful synthesis of these materials with unit cell parameters similar to the parent structure (Figures 3, S10-S13, S52-S55) Isolation of these materials, followed by subsequent solvent exchanges (DMF then DCM) affords MOFs with BET surface areas of 1989, 1427, 870 m²/g for Fe-MIL-101-butyrylamido, Fe-MIL-101-trimethylhexamido, and Fe-MIL-101-lauroylamido, respectively.

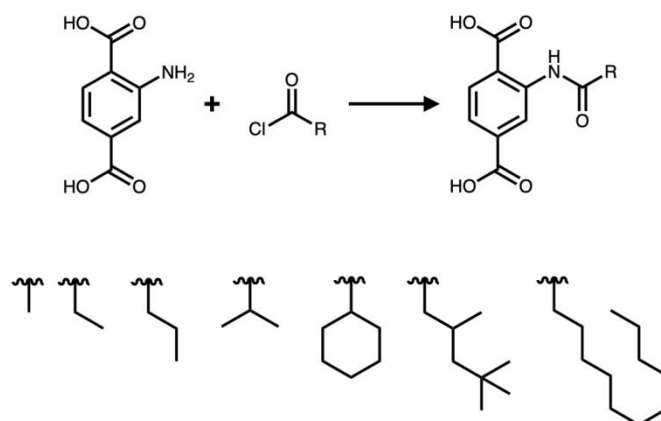


Fig. 2 The amide-based ligands used in this study where the reaction of 2-aminoterephthalic acid with acyl chlorides affords product in quantitative yield.

To assess the water stability of these materials, they were soaked in water for two weeks with samples removed for PXRD characterization at regular intervals. Although Fe-MIL-101-butyrylamido does lose crystallinity over the course of two weeks in DI H₂O, prominent peaks remain (Figures S16-S20). This increased stability is similarly observed at pH 2 and pH 5. The size of the butyryl groups decorating the pores of this material limits its water stability. The increased bulk of the methyl groups on the hexane functionalized material Fe-MIL-101-trimethylhexamido are expected to endow it with increased stability. Indeed, the sample exhibits only slight losses in crystallinity upon soaking in pH 2, 5, 8, or 11 solutions for as long as two weeks (Figures S26-S30). Similarly, the 12-carbon chains in Fe-MIL-101-lauroylamido result in hydrophobic pore surfaces and a relatively water-stable framework (Figure S21-S25).

In addition to increased stability to liquid water at various acid concentrations, the amide functionalization pursued here

can be used to tune the adsorption of water vapor in Fe-MIL-101 at room temperature. This has been a particularly active area of research over the past 5 years as MOFs have shown incredible utility for the production of pure water from arid environments.²⁶ The working pressures of MOFs in this application have been shown to be governed by the pore size and shape of the parent frameworks.²⁷ Amide-functionalization serves as a straightforward and facile method for tuning pore size. As compared to Fe-MIL-101, which becomes non-porous after exposure to water vapor, Fe-MIL-101-butyrylamido, Fe-MIL-101-trimethylhexanoylamido, and Fe-MIL-101-lauroylamido retain surface area and crystallinity after this treatment. Specifically, the BET surface areas of each material decrease from 1949 to 177, 1425 to 1124, and 929 to 480 m²/g, respectively. Consistent with the dramatic decrease in surface area for Fe-MIL-101-butyrylamido after water adsorption, subsequent H₂O adsorption isotherm experiments show decreased uptake under the same conditions. As the amide functionalization tunes the pore sizes of these materials (Figure S33) it not only limits the amount of surface area degradation displayed by each framework after water exposure, it drastically tunes the shape of the H₂O adsorption isotherm and its saturation capacity (Figure 3).

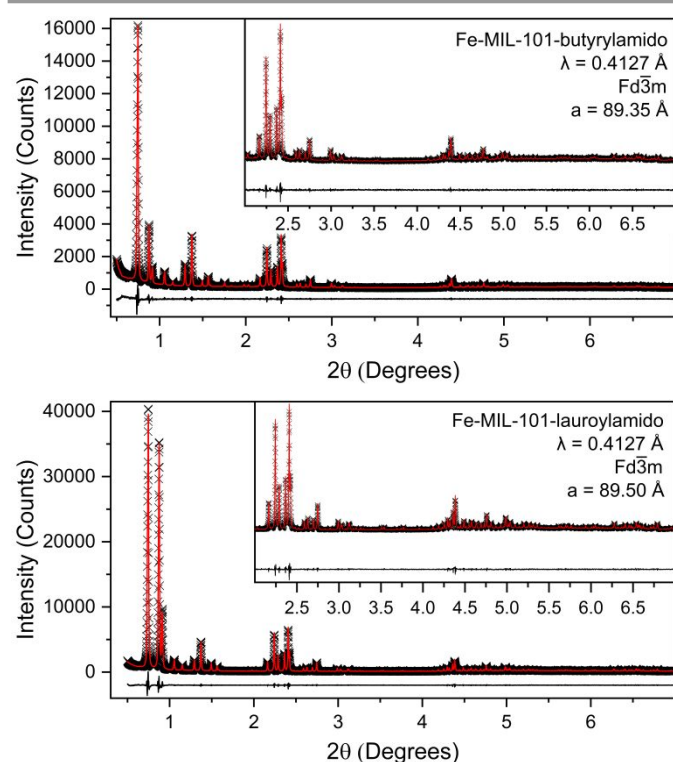


Fig. 3 Powder X-ray diffraction patterns of Fe-MIL-101-butyrylamido (top) and Fe-MIL-101-lauroylamido (bottom) with their respective unit cells.

The room temperature water adsorption isotherm for Fe-MIL-101 (Figure 4) displays a gradual increase in uptake to approximately $P/P_0 = 0.40$ where it sharply increases then plateaus until $P/P_0 = 0.80$ where it displays a sharp increase to a saturation capacity near 32 mmol/g. Upon installing functional groups, both the saturation uptake and position or presence of steps in the isotherms are tunable. For both the

trimethylhexanoyl- and lauroyl-functionalized MOFs, the pre-step uptake is decreased and the position of the step shifts above $P/P_0 = 0.38$. The vapor isotherms collected for both frameworks lack a second sharp uptake step and saturate near 15 mmol/g. The decreased saturation uptake is expected based on the decreased BET surface areas of both materials.

In an effort to fully tune water adsorption in Fe-MIL-101, we prepared a family of amide-functionalized frameworks featuring propionyl-, naphthoyl-, cyclohexanoyl-, and, phenyl-amido groups. The water isotherms of these materials (Figure 4) are substantially shifted as compared to those of Fe-MIL-101. The saturation uptake capacities of these frameworks generally correlate with Langmuir surface area. However, the shapes of the isotherms vary dramatically, particularly in the position of the steps that are present. The first abrupt step occurs at pressures ranging from $P/P_0 = 0.33$ - 0.40 while the second step is at $P/P_0 = 0.44$ - 0.59 . Importantly, the steps roughly correlate with pore size as determined from 77 K N₂ adsorption isotherm experiments.

As the bulky, alkyl-based functional groups that decorate the pores can be used to tune the stability and water adsorption properties of Fe-MIL-101, we also investigated their ability to tune phase. Fe³⁺ and terephthalic acid can combine to form multiple structures, including MIL-101, MIL-88, and MIL-53. While MIL-53 is based on 1-D channels of hydroxide-bridged iron cations, MIL-101 and MIL-88 are both based on trinuclear clusters featuring a μ_3 -O and six carboxylate ligands. The arrangement of these clusters in their structures is significantly altered (Figure 1). MIL-101 is highly porous and rigid while MIL-88 is a flexible material with lower surface area and pore volume. It is expected that the presence of large functional groups on the bridging ligand would disfavor the formation of MIL-88. Using the ligands reported here, any of the typical hydrothermal or solvothermal reaction routes we tested afforded MIL-101 as the favored phase. Changing the M:L ratio, pH, temperature, solvent, or any of the reaction parameters that have previously been shown to affect the phase of these structures had no discernible impact on phase of the product.

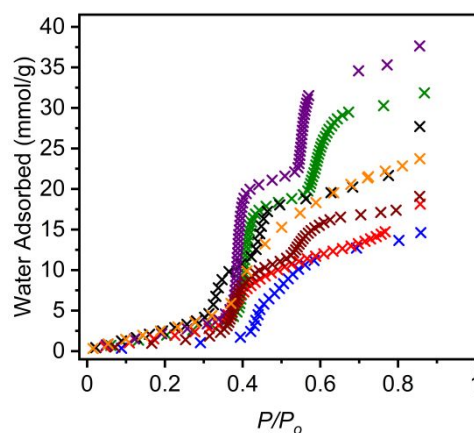


Fig. 4 Adsorption of water vapor in Fe-MIL-101-propionylamido (purple), Fe-MIL-101-butyrylamido (green), Fe-MIL-101-naphthoylamido (black), Fe-MIL-101-cyclohexanoylamido (orange), Fe-MIL-101-phenylamido (maroon), Fe-MIL-101-3,3,5-trimethylhexanoylamido (red) and Fe-MIL-101-lauroylamido (blue) samples at 25 °C.

We ultimately targeted the rate of delivery of Fe³⁺ to solution as a means to tune material phase. Iron metal, iron powder, or iron filings did not produce significant quantities of MOF over any useful reaction times. The leaching of iron from NdFeB magnets under acidic conditions has previously been employed to recycle the rare-earth portion.²⁸ With this in mind, we targeted the addition and/or utilization of NdFeB to reaction solutions as a means to slowly introduce iron cations into the reaction media. When ligands with amide groups containing four or more carbon atoms were used, MIL-101 was consistently isolated. Utilization of shorter ligands, however, allowed us to tune the phase of isolated MOF under various conditions. Under typical solvothermal conditions, the reaction of acetyl- or propionyl-amido functionalized H₂bdc in DMF with FeCl₃ affords highly crystalline MIL-101 (Figure S32). However, addition of NdFeB to the reaction mixture prior to heating affords MIL-88 for both ligands, as confirmed by PXRD (Figure S32).

For a subset of the ligands utilized here, product phase was observed prior to the application of heat. Indeed, the reaction of NdFeB with amide-functionalized ligands in DMF at room temperature produced significant quantities of MOF over 24 hours. Interestingly, the nature of the amide groups still had an impact on phase with MIL-101 being isolated upon reaction with butyryl, isobutyryl, and propanoyl-functionalized ligand while 2-acetylamidoterephthalic acid afforded MIL-88. Reaction of various iron(III) salts with ligands under similar conditions in the absence of NdFeB afforded no isolable solid after multiple weeks.

The work described here details the use of amide functionalized ligands to tune the water stability and phase of iron(III)-based metal-organic frameworks of the MIL-101 or MIL-88 structure types. This strategy, which also had a marked impact on water vapor adsorption at room temperature, should also be highly applicable to the highly-stable chromium(III) versions of these structure types. We also showed that the use of slow iron release via decomposition of iron-containing magnets afforded a level of control over phase and also facilitated the room temperature, salt free synthesis of these structures. Ongoing efforts in our lab are interested in elucidating the exact mechanism of NdFeB decomposition and subsequent MOF formation in the synthesis of MIL-101 and MIL-88 analogs.

This manuscript was prepared under cooperative agreement #70NANB17H302 from NIST, U.S. Department of Commerce. This work utilized facilities supported in part by the National Science Foundation under Agreement No. DMR-0944772. This work also used resources of the Advanced Photon Source; a U.S. Department of Energy (DOE) Office of Science User Facility operated for the DOE Office of Science by Argonne National Laboratory under Contract No. DE-AC02-06CH11357. We also thank the National Science Foundation for fellowship support of A.K.

Conflicts of interest

There are no conflicts to declare.

References

- (1) H. Furukawa, N. Ko, Y. B. Go, N. Aratani, B. S. Choi, E. Choi, A. O. Yazaydin, R. Q. Snurr, M. O'Keefe, J. Kim and O. M. Yaghi, *Science*, 2010, **329**, 424-428.
- (2) L. Hamon, C. Serre, T. Devic, T. Loiseau, F. Millange, G. Férey and G. D. Weireld, *J. Am. Chem. Soc.*, 2009, **131**, 8775-8777.
- (3) P. Rani and R. Srivastava, *New J. Chem.*, 2017, **41**, 8166-8177.
- (4) G. E. Cmarik, M. Kim, S. M. Cohen and K. S. Walton, *Langmuir*, 2012, **28**, 15606-15613.
- (5) K. O. Kirlikovali, Z. Chen, T. Islamoglu, J. T. Hupp and O. K. Farha, *ACS Appl. Mater. Interfaces*, 2020, **12**, 14702-14720.
- (6) S. Kitagawa, R. Kitaura and S. Noro, *Angew. Chem. Int. Ed.*, 2004, **43**, 2334-2375.
- (7) C. Volkringer, T. Loiseau, N. Guillou, G. Férey, E. Elkaim and A. Vimont, *Dalton Trans.*, 2009, 2241-2249.
- (8) S. Bernt, V. Guillerme, C. Serre and N. Stock, *Chem. Commun.*, 2011, **47**, 2838-2840.
- (9) J. Noh, Y. Kim, H. Park, J. Lee, M. Yoon, M. H. Park, Y. Kim, M. and Kim, *J. Ind. Eng. Chem.*, 2018, **64**, 478-483.
- (10) O. I. Lebedev, F. Millange, C. Serre, G. Van Tendeloo and G. Férey, *Chem. Mater.*, 2005, **17**, 6525-6527.
- (11) N. C. Burtch, H. Jasuja and K. S. Walton, *Chem. Rev.*, 2014, **114**, 10575-10612.
- (12) F. Serpaggi, T. Loiseau, F. Taulelle and G. Férey, *Microporous Mesoporous Mater.*, 1998, **20**, 197-206.
- (13) G. Férey, C. Mellot-Draznieks, C. Serre, F. Millange, J. Dutour, S. Surblé and L. Margiolako, *Science*, 2005, **309**, 2040-2042.
- (14) D. Y. Hong, Y. K. Hwang, C. Serre, G. Férey and J. -S. Chang, *Adv. Funct. Mater.*, 2009, **19**, 1537-1552.
- (15) T. Shen, J. Luo, S. Zhang and X. Luo, *J. Environ. Chem. Eng.*, 2015, **3**, 1372-1383.
- (16) S. Bhattacharjee, C. Chen and W. -S. Ahn, *RSC Adv.*, 2014, **4**, 52500-52525.
- (17) M. Bahri, F. Haghghat, H. Kazemian and S. Rohani, *Chem. Eng. J.*, 2017, **313**, 711-723.
- (18) P. Serra-Crespo, E. V. Ramos-Fernandez, J. Gascon and F. Kapteijn, *Chem. Mater.*, 2011, **23**, 2565-2572.
- (19) F. Carson, J. Su, A. E. Platero-Prats, W. Wan, Y. Yun, L. Samain and X. Zou, *Cryst. Growth Des.*, 2013, **13**, 5036-5044.
- (20) O. A. Kholdeeva, I. Y. Skobelev, I. D. Invachikova, K. A. Kovalenko, V. P. Fedin and A. B. Sorokin, *Catal. Today*, 2014, **238**, 54-61.
- (21) M. Lu, L. Li, S. Shen, D. Chen and W. Han, *New J. Chem.*, 2019, **43**, 1032-1037.
- (22) T. Ahnfeldt, D. Gunzelmann, T. Loiseau, D. Hirsemann, J. Senker, G. Férey and N. Stock, *Inorg. Chem.*, 2009, **48**, 3057-3064.
- (23) M. Kandiah, S. Usseglio, S. Svelle, U. Olsbye, K. P. Lillerud and M. Tilset, *J. Mater. Chem.*, 2010, **20**, 9848-9851.
- (24) A. D. S. Barbosa, D. Juliao, D. M. Fernandes, A. F. Peixoto, C. Freire, C. de Castro, S. S. Balula and L. Cunha-Silva, *Polyhedron*, 2017, **127**, 464-470.
- (25) D.-W. Kim, H.-G. Kim and D.-H. Cho, *Catal. Commun.*, 2016, **73**, 69-73.
- (26) W. Xu and O. M. Yaghi, *ACS Cent. Sci.* 2020, **6**, 8, 1348-1354.
- (27) J. Canivet, A. Fateeva, Y. Guo, B. Coasne and D. Farrusseng, *Chem. Soc. Rev.*, 2014, **43**, 5594-5617.
- (28) M. A. R. Onal, C. R. Borra, M. Guo, B. Blanpain and T. Van Gerven, *J. Rare Earths*, 2017, **35**, 574-584.